PHYSICAL REVIEW D VOLUME 19, NUMBER 3 1 FEBRUARY 1979

Gauge-model constraints of recent elastic and deep-inelastic neutral-current data

R. E. Hendrick* and Ling-Fong Li
Carnegie-Mellon University, Pittsburgh, Pennsylvania 15213
(Received 5 July 1978)

Recent neutrino-induced elastic and deep-inelastic neutral-current data are shown to impose stringent constraints on gauge models of weak interactions. For $SU_2 \times U_1$ models, assuming left-handed u and d quarks in a doublet, only the Weinberg-Salam model is in agreement with the data. $SU_2 \times SU_2 \times U_1$ and $SU_3 \times U_1$ models are also analyzed.

I. INTRODUCTION

One of the most important discoveries in recent years has been the existence of neutral currents in neutrino-induced reactions.[1] This discovery has given strong support to the description of weak and electromagnetic interactions in terms of spontaneously broken gauge theories.[2] Models proposed for a variety of theoretical reasons predict different quantitative results for neutral currents in neutrino reactions. Thus a careful study of neutral-current phenomenology can provide important clues to the detailed structure of gauge models of weak and electromagnetic interactions.

Recently, a second generation of accurate neutrino-induced neutral-current experiments has been completed. These experiments include the elastic neutrino- and antineutrino-proton scattering data recently reported by the Harvard-Pennsylvania-Wisconsin (HPW) collaboration,[3] and the neutral-current deep-inelastic scattering of neutrinos and antineutrinos on isoscalar targets measured by the CERN-Dortmund-Heidelberg-Saclay-Bologna (CDHSB) collaboration.[4] These data, summarized in Table I, will be shown to impose stringent phenomenological constraints on gauge models.

The most general effective Lagrangian, which describes ν_μ or $\bar{\nu}_\mu$ neutral-current scattering off hadrons, can be written as

$$\mathcal{L}_{\text{eff}} = G_Z/\sqrt{2}\,[\bar{\nu}_\mu \gamma_\lambda (1-\gamma_5)\nu_\mu] J_Z^\lambda . \tag{1.1}$$

where G_Z characterizes the overall strength of the neutral-current interactions and J_Z^λ is the part of the hadronic neutral-current coupling to the neutrino. In general, J_Z^λ contains light quarks (u and d) and heavy quarks ($s, c, \ldots$). We make the usual assumption that the nucleon matrix element of the heavy quarks is negligible compared with that of the light quarks. Then the part of J_Z^λ relevant to neutrinos scattering off a nucleon or nucleus target can be parameterized as

$$J_Z^\lambda = a_L(u)\bar{u}\gamma^\lambda(1-\gamma_5)u + a_L(d)\bar{d}\gamma^\lambda(1-\gamma_5)d + a_R(u)\bar{u}\gamma^\lambda(1+\gamma_5)u + a_R(d)\bar{d}\gamma^\lambda(1+\gamma_5)d , \tag{1.2}$$

where $q_{iL} = \frac{1}{2}(1-\gamma_5)q_i$ and $q_{iR} = \frac{1}{2}(1+\gamma_5)q_i$ are left-handed and right-handed components of the quark fields. The parameters $a_{L,R}(q_i)$ characterize the strength of each piece of the neutral current. Experimental data on neutral-current reactions involving neutrinos allow us to measure these four coupling constants: $a_L(u)$, $a_L(d)$, $a_R(u)$, and $a_R(d)$.

A number of authors, most recently Abbott and Barnett,[5] have made use of neutral-current neutrino data to fix these coupling parameters. Abbott and Barnett used not only the elastic and deep-inelastic neutrino data, but also included both inclusive and exclusive pion-production data. Most other recent phenomenological analyses[6-9] also make use of the one-pion inclusive production data. However, the analysis of pion production in neutrino neutral-current reactions requires additional theoretical assumptions about the pion-production mechanism. The inclusive pion analysis uses the parton model at rather low energies as well as assumptions about the pion-fragmentation mechanism.[10] Exclusive pion analysis at low-energies uses a detailed model of resonant and nonresonant pion production.[11]

In this paper, we present a determination of couplings based only on the recently measured elastic and deep-inelastic neutrino-induced neutral-current data, summarized in Table I. It should be noted that the q^2 cuts and cross sections for the elastic scattering data have changed since the analysis of Abbott and Barnett.[5] Of course, even the analysis of elastic and deep-inelastic neutral-current data is not free from theoretical input, though that input is on a much firmer footing than the pion-production assumptions. In elastic $\nu_\mu p$ and $\bar{\nu}_\mu p$ scattering we assume that the ratio of isoscalar to isovector form factors for axial-vector currents is given by SU_3. To the extent

TABLE I. Summary of elastic and deep-inelastic neutrino-induced neutral-current data from experiments of Columbia-Illinois-Rockefeller (CIR), HPW (Harvard-Pennsylvania-Wisconsin (HPW), Harvard-Pennsylvania-Wisconsin-Fermilab (HPWF), Caltech-Fermilab (CF), Gargamelle, and CERN-Dortmund-Heidelberg-Saclay-Bologna (CDHSB) collaborations.

Elastic data \ Experiment	CIR	HPW (1st generation)	HPW (2nd generation)
$R_{\rm el}^{\nu}=\frac{\sigma_{\nu p\to\nu p}}{\sigma_{\nu n\to\mu^- p}}$	0.23 ± 0.09	0.17 ± 0.05	0.11 ± 0.02
$R_{\rm el}^{\bar\nu}=\frac{\sigma_{\bar\nu n\to\bar\nu p}}{\sigma_{\bar\nu p\to\mu^+ n}}$		0.20 ± 0.10	0.19 ± 0.05

Inclusive data \ Experiment	HPWF	CF	Gargamelle	CDHSB
$R^{\nu}=\frac{\sigma_{\nu N\to\nu X}^{\rm nc}}{\sigma_{\nu N\to\mu^- X}^{\rm cc}}$	0.29 ± 0.04 $\langle E_\nu\rangle\simeq 53$ GeV	0.24 ± 0.04 $\langle E_\nu\rangle\simeq 50$ GeV	0.25 ± 0.04 $\langle E_\nu\rangle\simeq 2$ GeV	0.295 ± 0.010 $12\le E_\nu\le 200$ GeV
$R^{\bar\nu}=\frac{\sigma_{\bar\nu N\to\bar\nu X}^{\rm nc}}{\sigma_{\bar\nu N\to\mu^+ X}^{\rm cc}}$	0.39 ± 0.10 $\langle E_{\bar\nu}\rangle\simeq 41$ GeV	0.35 ± 0.11 $\langle E_{\bar\nu}\rangle\simeq 50$ GeV	0.39 ± 0.06 $\langle E_{\bar\nu}\rangle\simeq 2$ GeV	0.34 ± 0.03 $12\le E_{\bar\nu}\le 200$ GeV
$R_{\rm cc}=\frac{\sigma_{\bar\nu N\to\mu^+ X}^{\rm cc}}{\sigma_{\nu N\to\mu^- X}^{\rm cc}}$			0.38 ± 0.02	0.48 ± 0.025

that strange-quark contributions may be ignored, this assumption is justified. In analyzing CDHSB deep-inelastic neutrino scattering data we assume validity of the parton model.[12] The energies of the CDHSB data are certainly high enough to permit such an assumption.

The analysis in this paper has been done in such a way as to reveal correlations among relevant parameters. In determining the constraints on the coupling parameters $a_L(u)$, $a_L(d)$, $a_R(u)$, and $a_R(d)$ due to the elastic and inclusive data, for example, we include correlations between left- and right-handed couplings.

In analyzing $SU_2\times U_1$ gauge models we have assumed that left-handed quarks belong to the weak-isospin doublet

$$\begin{pmatrix} u \\ d \end{pmatrix}_L, \quad T_3(u_L)=\tfrac{1}{2}, \quad T_3(d_L)=-\tfrac{1}{2}. \tag{1.3}$$

We then examine the constraints the elastic and inclusive neutrino data place on the remaining four free parameters: $T_3(u_R)$ and $T_3(d_R)$, the weak isospins of the right-handed u and d quarks, $\sin^2\theta_W$, the Weinberg angle, and λ, a fourth free parameter multiplying neutral-current cross sections arising from a free choice of Higgs bosons. The general class of $SU_2\times U_1$ models consistent with the assignment of Eq. (1.3) is examined, as well as a number of specific $SU_2\times SU_2\times U_1$ and $SU_3\times U_1$ models.

We find that without using inclusive or exclusive pion-production analyses the recent elastic and deep-inelastic neutral-current results are accurate enough to provide a useful test of various gauge models. Within the class of $SU_2\times U_1$ models consistent with Eq. (1.3), only the Weinberg-Salam[2] (WS) model agrees with these data within 1 standard deviation for any value of the Weinberg angle and λ. Since the $SU_2\times SU_2\times U_1$ model of Mohapatra and Sidhu[13] reproduces the phenomenology of the WS model for $\epsilon=0$, it too has a region of agreement within 1 standard deviation. The $SU_3\times U_1$ model of Lee and Weinberg[14] is found to have a range of parameters within 2 standard deviations; the model of Langacker and Segre[15] is not consistent with the elastic and deep-inelastic data within 3 standard deviations.

Section II of this paper discusses our analysis of elastic neutral-current scattering, Sec. III details our analysis of inclusive neutral-current neutrino-induced scattering. In Sec. IV we discuss our analysis and results, and Sec. V contains our conclusions.

II. ELASTIC NEUTRAL-CURRENT SCATTERING

The differential cross section for elastic ν or $\bar\nu$ scattering on protons can be expressed in terms of the form factors of the neutral current J_Z^λ as (see Fig. 1)

$$\frac{d\sigma^{(\nu,\bar\nu)}}{dQ^2}=\frac{G_Z^2}{2\pi}\left\{\frac{G_E^2}{1+\tau}\left[\left(1-\frac{M}{E}\tau\right)^2-\left(\frac{M}{E}\right)^2\tau(\tau+1)\right]+\left(\frac{G_M^2\tau}{1+\tau}+G_A^2\right)\left[\left(1-\frac{M}{E}\tau\right)^2+\tau(\tau+1)\left(\frac{M}{E}\right)^2\right]\pm 4\tau\left(\frac{M}{E}\right)\left(1-\frac{M}{E}\tau\right)G_M G_A\right\}, \tag{2.1}$$

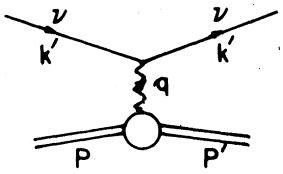

FIG. 1. Lowest-order graph contributing to ν- (or $\bar{\nu}$-) proton elastic scattering.

with $Q^2=-q^2=(k-k')^2$, $\tau=Q^2/4M^2$, and M is the nucleon mass.

The form factors, G_E, G_M, and G_A, defined by

$$\begin{aligned}\langle P'|J_\mu^Z|p\rangle &= \bar{u}(p')\left[\gamma_\mu F_1(q^2)+\frac{i\sigma_{\mu\nu}q^\nu}{2M}F_2(q^2)\right.\\ &\quad\left.+\gamma_5\gamma_\mu G_A(q^2)\right]u(p)\,,\\ G_E(q^2)&=F_1(q^2)+\frac{q^2}{4M^2}F_2(q^2)\,,\\ G_M(q^2)&=F_1(q^2)+F_2(q^2)\end{aligned}\tag{2.2}$$

are the usual electric and magnetic form factors for the vector current, and $G_A(q^2)$ is the usual axial-vector form factor. It is convenient to decompose the current J_μ^Z by Lorentz and isospin properties into

$$J_\mu^Z=\epsilon_V^{(0)}V_\mu^{(0)}+\epsilon_V^{(1)}V_\mu^{(1)}+\epsilon_A^{(0)}A_\mu^{(0)}+\epsilon_A^{(1)}A_\mu^{(1)}\,,\tag{2.3}$$

where

$$\begin{aligned}V_\mu^{(0)}&=\tfrac{1}{2}(\bar{u}\gamma_\mu u+\bar{d}\gamma_\mu d)\,,\\ V_\mu^{(1)}&=\tfrac{1}{2}(\bar{u}\gamma_\mu u-\bar{d}\gamma_\mu d)\end{aligned}\tag{2.4}$$

are the isoscalar and isovector currents, and

$$\begin{aligned}A_\mu^{(0)}&=\tfrac{1}{2}(\bar{u}\gamma_5\gamma_\mu u+\bar{d}\gamma_5\gamma_\mu d)\,,\\ A_\mu^{(1)}&=\tfrac{1}{2}(\bar{u}\gamma_5\gamma_\mu u-\bar{d}\gamma_5\gamma_\mu d)\end{aligned}\tag{2.5}$$

are the corresponding axial-vector currents.

The coefficients $\epsilon_{V,A}^{(0)}$ and $\epsilon_{V,A}^{(1)}$ are given by

$$\begin{aligned}\epsilon_V^{(0)}&=a_L(u)+a_R(u)+a_L(d)+a_R(d)\,,\\ \epsilon_V^{(1)}&=a_L(u)+a_R(u)-a_L(d)-a_R(d)\\ \epsilon_A^{(0)}&=a_L(u)-a_R(u)+a_L(d)-a_R(d)\,,\\ \epsilon_A^{(1)}&=a_L(u)-a_R(u)-a_L(d)+a_R(d)\,.\end{aligned}\tag{2.6}$$

Assuming that the nucleon matrix elements of the heavy quarks are negligible, the hadronic electromagnetic current can be written as

$$J_\lambda^{em}=\tfrac{1}{3}(2\bar{u}\gamma_\lambda u-\bar{d}\gamma_\lambda d)=V_\lambda^{(1)}+\tfrac{1}{3}V_\lambda^{(0)}\,.\tag{2.7}$$

The nucleon form factors of J_λ^{em} are well-known experimentally to satisfy the scaling law, i.e.,

$$\begin{aligned}G_{E_p}^{em}(q^2)&=\frac{G_{M_p}^{em}(q^2)}{\mu_p}=\frac{G_{M_n}^{em}(q^2)}{\mu_n}=\frac{1}{(1-q^2/M_V^2)^2}\,,\\ M_V^2&=0.71\ \text{GeV}^2\,,\\ G_{E_n}^{em}(q^2)&=0\end{aligned}\tag{2.8}$$

where $\mu_p=2.79$ and $\mu_n=-1.91$ are the anomalous magnetic moments of the proton and the neutron, respectively. Then the vector form factors G_E and G_M of the hadronic neutral current J_λ^Z can be related to those of J_λ^{em} through the isospin property

$$\begin{aligned}G_E&=\tfrac{1}{2}(3\epsilon_V^{(0)}+\epsilon_V^{(1)})G_{E_p}\\ &=\tfrac{1}{2}(3\epsilon_V^{(0)}+\epsilon_V^{(1)})\frac{1}{(1-q^2/M_V^2)^2}=\frac{\gamma_E}{(1-q^2/M_V^2)^2}\,,\\ \gamma_E&=\tfrac{1}{2}(3\epsilon_V^{(0)}+\epsilon_V^{(1)})\end{aligned}\tag{2.9}$$

$$\begin{aligned}G_M&=\tfrac{1}{2}[3\epsilon_V^{(0)}(\mu_p+\mu_n)+\epsilon_V^{(1)}(\mu_p-\mu_n)]\frac{1}{(1-q^2/M_V^2)^2}\\ &=\tfrac{1}{2}(2.64\epsilon_V^{(0)}+4.7\epsilon_V^{(1)})\\ &\quad\times\frac{1}{(1-q^2/M_V^2)^2}=\frac{\gamma_M}{(1-q^2/M_V^2)^2}\,,\\ \gamma_M&=\tfrac{1}{2}(2.64\epsilon_V^{(0)}+4.7\epsilon_V^{(1)})\,.\end{aligned}\tag{2.10}$$

For the axial-vector current, we define the isovector and isoscalar form factors by

$$\begin{aligned}\langle p|A_\mu^{(1)}|p\rangle&=\tfrac{1}{2}G_A^{(1)}(q^2)\bar{u}_p\gamma_5\gamma_\mu u_p\,,\\ \langle p|A_\mu^{(0)}|p\rangle&=\tfrac{1}{2}G_A^{(0)}(q^2)\bar{u}_p\gamma_5\gamma_\mu u_p\,.\end{aligned}\tag{2.11}$$

The isovector form factor $G_A^{(1)}$ can be related to the charged axial-vector form factor measured in the reaction $\nu_\mu+n\to\mu^-+p$, with the result[16]

$$G_A^{(1)}(q^2)=\frac{1.24}{(1-q^2/M_A^2)^2},\quad M_A^2=0.90\ \text{GeV}^2\,.\tag{2.12}$$

For lack of experimental knowledge about the isoscalar axial form factor, we will assume that the isoscalar axial form factor $G_A^{(0)}(q^2)$ has the same q^2 dependence as the isovector axial form factor $G_A^{(1)}(q^2)$, i.e.,

$$G_A^{(0)}(q^2)=kG_A^{(1)}(q^2)\,.$$

Within the assumption that the nucleon matrix elements of heavy quarks can be neglected, we can use SU(3) symmetry to relate the proportionality constant k to the D/F ratio,[17]

$$k=3-4\alpha_A,\quad\text{where }\alpha_A=D/(F+D)\,.$$

Experimentally,[18] $\alpha_A=0.658\pm0.007$, and hence we take the isoscalar axial form factor to be of the

form

$$G_A^{(0)}(q^2) = 0.368 G_A^{(1)}.$$

The total axial form factor is then

$$G_A(q^2) = \tfrac{1}{2}[\epsilon_A^{(1)} G_A^{(1)}(q^2) + \epsilon_A^{(0)} G_A^{(0)}(q^2)] = \frac{1.24\gamma_A}{(1 - q^2/M_A{}^2)^2}, \tag{2.13}$$

where

$$\gamma_A = \tfrac{1}{2}(\epsilon_A^{(1)} + 0.368\epsilon_A^{(0)}). \tag{2.14}$$

With these expressions for the form factors G_E, G_M, and G_A, we can rewrite the differential cross section in (2.2) as

$$\frac{d\sigma^{(\nu,\bar\nu)}}{dQ^2} = \frac{G_Z{}^2}{2\pi}[\gamma_E{}^2 f_1(Q^2,E) + \gamma_M{}^2 f_2(Q^2,E) + \gamma_A{}^2 f_3(Q^2,E) \pm \gamma_A\gamma_M f_4(Q^2,E)], \tag{2.15}$$

where the kinematical functions $f_i(Q^2,E)$ are given by

$$f_1(Q^2,E) = \frac{1}{(1+Q^2/M_V{}^2)^4}\left[\left(\frac{1}{1+\tau}\right)\left(1-\tau\frac{M}{E}\right)^2 - \tau\left(\frac{M}{E}\right)^2\right],$$

$$f_2(Q^2,E) = \frac{1}{(1+Q^2/M_V{}^2)^4}\left[\frac{\tau}{1+\tau}\left(1-\tau\frac{M}{E}\right)^2 + \tau^2\left(\frac{M}{E}\right)^2\right], \tag{2.16}$$

$$f_3(Q^2,E) = \frac{(1.24)^2}{(1+Q^2/M_A{}^2)^4}\left[\left(1-\frac{M}{E}\tau\right)^2 + \tau(1+\tau)\left(\frac{M}{E}\right)^2\right],$$

$$f_4(Q^2,E) = 4\tau\left(\frac{M}{E}\right)\left(1-\tau\frac{M}{E}\right)\frac{1}{(1+Q^2/M_V{}^2)^2} \times \frac{1.24}{(1+Q^2/M_A{}^2)^2}.$$

In Eq. (2.15), $f_i(Q^2,E)$ are the model-independent kinematical functions of Q^2 and E; all the model dependence is contained in the constant coefficients γ_E, γ_M, and γ_A. Hence, in principle, for any model which predicts the values of the coefficients γ_E, γ_M, and γ_A, we can use Eq. (2.15) to work out the differential cross section $d\sigma/dQ^2$ and fold it with the ν or $\bar\nu$ spectrum[19] to compare with experimental data (since broad band ν or $\bar\nu$ beams are used in the experiments). All the Q^2 dependent is contained in the known kinematical functions $f_i(Q^2,E)$. To compare to the experimental data, we integrate the differential cross section over Q^2 subject to the HPW experimental cut $0.4 < Q^2 < 0.9$, integrating over the neutrino or antineutrino spectra, and normalizing to the charged-current cross sections, giving

$$R_{el}^{\nu} = \frac{\sigma(\nu p \to \nu p)}{\sigma(\nu n \to \mu^- p)} = \lambda(F_1\gamma_E{}^2 + F_2\gamma_M{}^2 + F_3\gamma_A{}^2 + F_4\gamma_A\gamma_M), \tag{2.17}$$

$$R_{el}^{\bar\nu} = \frac{\sigma(\bar\nu p \to \bar\nu p)}{\sigma(\bar\nu p \to \mu^+ n)} = \lambda(\bar F_1\gamma_E{}^2 + \bar F_2\gamma_M{}^2 + \bar F_3\gamma_A{}^2 - \bar F_4\gamma_A\gamma_M), \tag{2.18}$$

where

$$\begin{pmatrix} F_i \\ \bar F_i \end{pmatrix} = \frac{G_F{}^2}{2\pi}\int_{0.4}^{0.9} dQ^2 \int dE \begin{pmatrix} g_\nu(E)/\sigma(\nu n \to \mu^- p) \\ g_{\bar\nu}(E)/\sigma(\bar\nu p \to \mu^+ n) \end{pmatrix} \times f_i(Q^2,E). \tag{2.19}$$

$g_\nu(E)$ and $g_{\bar\nu}(E)$ are the BNL spectra for ν and $\bar\nu$, and $\lambda = G_Z{}^2/G_F{}^2$. If we take $M_A{}^2 = 0.90$ (GeV)^2, then F_i and $\bar F_i$ are given by

$$F_1 = 0.070, \quad F_2 = 0.017, \quad F_3 = 0.266, \quad F_4 = 0.079$$

$$\bar F_1 = 0.234, \quad \bar F_2 = 0.058, \quad \bar F_3 = 0.930, \quad \bar F_4 = 0.291.$$

Equations (2.17) and (2.18), then read

$$R_{el}^{\nu} = \lambda(0.070\gamma_E{}^2 + 0.017\gamma_M{}^2 + 0.266\gamma_A{}^2 + 0.079\gamma_A\gamma_M), \tag{2.20}$$

$$R_{el}^{\bar\nu} = \lambda(0.234\gamma_E{}^2 + 0.058\gamma_M{}^2 + 0.930\gamma_A{}^2 - 0.291\gamma_A\gamma_M). \tag{2.21}$$

In these forms, the experimental data on R_{el}^{ν} and $R_{el}^{\bar\nu}$ will give model-independent relations among the parameters γ_E, γ_M, γ_A, and λ. If we take into account the experimental uncertainties in R_{el} and $R_{el}^{\bar\nu}$, Eqs. (2.20) and (2.21) will give two constraints among the parameters rather than exact relations. These constraints can be used along with inclusive cross-section constraints to test the validity of each model.

Let us first consider gauge models based on the SU(2)$\times$U(1) group. In this simple case, there is only one neutral current given by

$$J_\lambda^Z = 2\sum_i \{\bar q_{iL}\gamma_\lambda[T_3(q_{iL}) - Q(q_{iL})\sin^2\theta_W]q_{iL} + \bar q_{iR}\gamma_\lambda[T_3(q_{iR}) - Q(q_{iR})\sin^2\theta_W]q_{iR}\}, \tag{2.22}$$

where θ_W is the Weinberg angle, $Q(q_i)$ is the charge of q_i, and $T_3(q_{iL})$ is the 3rd component of the weak isospin of q_{iL}. The basic neutral-current Lagrangian is given by

$$\mathfrak{L}_{nc} = \frac{g}{2\cos\theta_W} Z^\mu (J_\mu^Z + J_\mu^{lZ}), \tag{2.23}$$

where $J_\lambda^{lZ} = \bar\nu_{\mu L}\gamma_\lambda\nu_{\mu L} + \cdots$ is the leptonic neutral current. Comparing with the second-order effec-

tive Lagrangian given in Eq. (2.1), we can identify

$$G_Z/\sqrt{2} = \frac{g^2}{8\cos^2\theta_W M_Z{}^2}.$$

From the charged-current interaction, we get

$$\lambda = \left(\frac{G_Z}{G_F}\right)^2 = \left(\frac{M_W{}^2}{M_Z{}^2\cos^2\theta_W}\right)^2, \quad G_F/\sqrt{2} = \frac{g^2}{8M_W{}^2}. \tag{2.24}$$

For the simple case where only the doublet Higgs field is present, we have $M_W{}^2 = M_Z{}^2\cos^2\theta_W$, which gives $\lambda = 1$. For more general models with both triplet and doublet Higgs fields λ can be arbitrary. However, the result of combined analysis of elastic and inelastic neutral-current $\bar{\nu}$ and ν reactions show that $\lambda \simeq 1$ seems to be preferred. Our analysis does not assume a value for λ.

Most models based on the SU(2) × U(1) group assume the left-handed quark fields (u_L, d_L, s_L, and c_L) are in doublets,

$$\begin{pmatrix} u \\ d_C \end{pmatrix}_L, \quad \begin{pmatrix} c \\ s_C \end{pmatrix}_L$$

where

$$d_C = \cos\theta_C d + \sin\theta_C s,$$

$$s_C = -\sin\theta_C d + \cos\theta_C s,$$

and θ_C is the Cabibbo angle. Therefore, most models based on SU(2) × U(1) can be classified according to the possible assignments of right-handed components of the light-quark fields, u_R, d_R. Some of the possible models, which are characterized by the values of $T_3(u_R)$ and $T_3(d_R)$, are listed in Table II. In general, there will be mixing between states with the same charge and helicity. For simplicity, we assume the mixing angles to be negligible. Then, from the structure of the hadronic neutral current given in Eq. (2.22), we can read out the coefficients $\epsilon_{V,A}^{(0)}$ and $\epsilon_{V,A}^{(1)}$,

$$\begin{aligned} \epsilon_V^{(0)} &= T_3(u_R) + T_3(d_R) - \tfrac{2}{3}\sin^2\theta_W, \\ \epsilon_V^{(1)} &= T_3(u_R) - T_3(d_R) - 2\sin^2\theta_W + 1, \\ \epsilon_A^{(0)} &= -T_3(u_R) - T_3(d_R), \\ \epsilon_A^{(1)} &= 1 - T_3(u_R) + T_3(d_R). \end{aligned} \tag{2.25}$$

We then may express the cross-section ratios R_{el}^{ν} and $R_{el}^{\bar{\nu}}$ as functions of $T_3(u_R)$, $T_3(d_R)$, the Weinberg angle, and λ.

The $SU_2 \times SU_2 \times U_1$ model of Mohapatra and Sid-

TABLE II. Classification of SU(2) × U(1) gauge models according to weak isospin of right-handed quarks.

Model	Right-handed multiplet structure	$T_3(u_R)$ (x coordinate in Fig. 5)	$T_3(d_R)$ (y coordinate in Fig. 5)
Weinberg-Salam	$(u)_R, (d)_R, \cdots$	0	0
b quark	$\begin{pmatrix} u \\ b \end{pmatrix}_R, (d)_R, \cdots$	$\frac{1}{2}$	0
t quark	$(u)_R, \begin{pmatrix} t \\ d \end{pmatrix}_R, \cdots$	0	$-\frac{1}{2}$
Vector	$\begin{pmatrix} u \\ b \end{pmatrix}_R, \begin{pmatrix} t \\ d \end{pmatrix}_R, \cdots$	$\frac{1}{2}$	$-\frac{1}{2}$
Unconventional models:	$(u)_R, \begin{pmatrix} d \\ a \end{pmatrix}_R, \cdots$	0	$\frac{1}{2}$
	$\begin{pmatrix} v \\ u \end{pmatrix}_R, (d)_R, \cdots$	$-\frac{1}{2}$	0
	$\begin{pmatrix} v \\ u \end{pmatrix}_R, \begin{pmatrix} d \\ a \end{pmatrix}_R, \cdots$	$-\frac{1}{2}$	$\frac{1}{2}$
	$\begin{pmatrix} v \\ u \end{pmatrix}_R, \begin{pmatrix} t \\ d \end{pmatrix}_R, \cdots$	$-\frac{1}{2}$	$-\frac{1}{2}$
	$\begin{pmatrix} u \\ v \\ w \end{pmatrix}_R, (d)_R, \cdots$	1	0

hu, designed to provide naturally parity conserving neutral currents, assigns u and d quarks to left-handed and right-handed doublets transforming under separate SU_2 groups. The relevant neutral-current phenomenology depends on two adjustable parameters, ϵ and x, with[20]

$$\begin{aligned}
\epsilon_L(u) &= \tfrac{1}{4}\left(\frac{1-\frac{4}{3}x}{1-\epsilon}+\frac{1}{1+\epsilon}\right),\\
\epsilon_L(d) &= \tfrac{1}{4}\left(\frac{-1+\frac{2}{3}x}{1-\epsilon}-\frac{1}{1+\epsilon}\right),\\
\epsilon_R(u) &= \tfrac{1}{4}\left(\frac{1-\frac{4}{3}x}{1-\epsilon}+\frac{1}{1+\epsilon}\right),\\
\epsilon_R(d) &= \tfrac{1}{4}\left(\frac{-1+\frac{2}{3}x}{1-\epsilon}+\frac{1}{1+\epsilon}\right).
\end{aligned} \tag{2.26}$$

The Mohapatra-Sidhu model reproduces the neutral-current phenomenology of the Weinberg-Salam model for $\epsilon = 0$, $x = 2\sin^2\theta_W$. In general, $-1 < \epsilon < 1$ and $x > 0$.

There are several popular $SU_3 \times U_1$ models assigning left- and right-handed quarks to weak-SU_3 triplets. The model of Lee and Weinberg[14] assigns quarks to the multiplets

$$\begin{pmatrix} u \\ d \\ b \end{pmatrix}_L , \quad \begin{pmatrix} t \\ b \\ d \end{pmatrix}_R , \quad u_R .$$

Neutral-current scattering depends on two adjustable parameters, l and w, $l \geq 0$, $0 \leq w \leq 1$, with[20]

$$\begin{aligned}
\epsilon_L(u) &= \tfrac{1}{2}(1+l)(1-w),\\
\epsilon_L(d) &= \tfrac{1}{4}(1+l)(-1+w),\\
\epsilon_R(u) &= -\tfrac{1}{2}(1+l)w,\\
\epsilon_R(d) &= \tfrac{1}{4}(1+l)(-1+w).
\end{aligned} \tag{2.27}$$

The model of Langacker and Segrè[15] assigns quarks to the triplets

$$\begin{pmatrix} u \\ d \\ b \end{pmatrix}_L , \quad \begin{pmatrix} u \\ b \\ d \end{pmatrix}_R .$$

Phenomenological predictions again depend on two parameters, r' and r'', which depend on ratios of Higgs parameters and the Weinberg angle, ranging roughly over the values $\frac{1}{2} \leq r' \leq 1$ and $r'' \geq 0$. In this model,[20]

$$\begin{aligned}
\epsilon_L(u) &= r''/2,\\
\epsilon_L(d) &= -\tfrac{1}{4}(r''+r'),\\
\epsilon_R(u) &= r''/2,\\
\epsilon_R(d) &= -\tfrac{1}{4}(r''-r').
\end{aligned} \tag{2.28}$$

III. INCLUSIVE NEUTRAL-CURRENT SCATTERING

Here we summarize gauge-model parametrizations of deep-inelastic neutral-current scattering to compare with the experimental measurements of neutrinos scattering on isoscalar targets (Fig. 2).

An essential assumption in the analysis of deep-inelastic scattering is the parton model.[12] In the usual quark-parton picture, the lepton-hadron deep-inelastic cross section can be expressed in terms of quark distribution functions $q_i(x)$, with $x = q^2/2M\nu$. Since the charged current ν and $\bar{\nu}$ inclusive cross sections are very well described by the usual left-handed doublets in the WS model, i.e.,

$$\begin{pmatrix} u \\ d_C \end{pmatrix}_L , \quad \begin{pmatrix} c \\ s_C \end{pmatrix}_L ,$$

we will assume that for the models with right-handed currents, the new quarks to which u_R or d_R couples are very heavy, so that they do not contribute to the present day experiments. Thus for the isoscalar target, the charged current ν or $\bar{\nu}$ inclusive cross sections are given by

$$\begin{aligned}
\sigma_{cc}^{\nu} &= \sigma(\nu N \to \mu^- X)\\
&= (G_F^2 ME/\pi)\int_0^1 x\,dx\{[u(x)+d(x)]+\tfrac{1}{3}[\bar{u}(x)+\bar{d}(x)]\},
\end{aligned} \tag{3.1}$$

$$\begin{aligned}
\sigma_{cc}^{\bar{\nu}} &= \sigma(\bar{\nu} N \to \mu^+ X)\\
&= (G_F^2 ME/\pi)\int_0^1 x\,dx\{[\bar{u}(x)+\bar{d}(x)]+\tfrac{1}{3}[u(x)+d(x)]\},
\end{aligned} \tag{3.2}$$

where $u(x)$, $d(x)$ and $\bar{u}(x)$, $\bar{d}(x)$ are the usual quark and antiquark distribution functions.

For convenience, we will use the notation

$$q(x) = \tfrac{1}{2}[u(x)+d(x)], \tag{3.3}$$

to write

$$R_{cc} = \frac{\sigma_{cc}^{\bar{\nu}}}{\sigma_{cc}^{\nu}} = \frac{\int_0^1 x\,dx\,[\bar{q}(x)+\frac{1}{3}q(x)]}{\int_0^1 x\,dx\,[q(x)+\frac{1}{3}\bar{q}(x)]} . \tag{3.4}$$

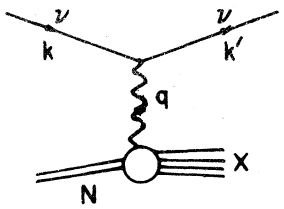

FIG. 2. Lowest-order graph for ν- (or $\bar{\nu}$-) induced deep-inelastic neutral-current scattering.

From the CDHSB experiment, we use the result[21]

$$R_{cc} = 0.48 \pm 0.025 . \tag{3.5}$$

For the general neutral-current parameterized in Eq. (1.2), the ν neutral-current inclusive cross section on the isoscalar target, is given by

$$\sigma^{\nu}_{nc} = \frac{2\lambda G_F^2 ME}{\pi} [a_L^2(u) + a_L^2(d)] \int_0^1 x\,dx [q(x) + \tfrac{1}{3}\bar{q}(x)] + [a_R^2(u) + a_R^2(d)] \int_0^1 x dx [\bar{q}(x) + \tfrac{1}{3} q(x)] . \tag{3.6}$$

If we normalize it to the corresponding charged-current inclusive cross section and use the relation (3.4), we obtain

$$R^{\nu} = \frac{\sigma^{\nu}_{nc}}{\sigma^{\nu}_{cc}} = \lambda\{[a_L^2(u) + a_L^2(d)] + R_{cc}[a_R^2(u) + a_R^2(d)]\} . \tag{3.7}$$

Similarly, for $\bar{\nu}$ neutral-current inclusive cross section, we obtain

$$R^{\bar{\nu}} = \frac{\sigma^{\bar{\nu}}_{nc}}{\sigma^{\bar{\nu}}_{cc}} = \lambda\{[a_L^2(u) + a_L^2(d)] + R_{cc}^{-1}[a_R^2(u) + a_R^2(d)]\} . \tag{3.8}$$

From the measured values of R^{ν}, $R^{\bar{\nu}}$, and R_{cc}, Eqs. (3.7) and (3.8) give relations among the parameters $a_L(u)$, $a_L(d)$, $a_R(u)$, $a_R(d)$, and λ. Before comparing with the predictions of various models, we first separate the right-handed couplings from the left-handed couplings by forming the following combinations out of Eqs. (3.7) and (3.8):

$$A = \frac{R_{cc}^{-1} R^{\nu} - R_{cc} R^{\bar{\nu}}}{R_{cc}^{-1} - R_{cc}} = \lambda[a_L^2(u) + a_L^2(d)] = \epsilon_L^2(u) + \epsilon_L^2(d) \tag{3.9}$$

$$B = \frac{R^{\bar{\nu}} - R^{\nu}}{R_{cc}^{-1} - R_{cc}} = \lambda[a_R^2(u) + a_R^2(d)] = \epsilon_R^2(u) + \epsilon_R^2(d) . \tag{3.10}$$

where $\epsilon_L(q_i) = \lambda^{1/2} a_L(q_i)$.

For the SU(2)× U(1) gauge models considered in the last section, which have common left-handed doublets but with different assignments for u_R and d_R, we have the following values for the parameters:

$$a_L(u) = \tfrac{1}{2} - \tfrac{2}{3}\sin^2\theta_W , \tag{3.11a}$$

$$a_L(d) = -\tfrac{1}{2} + \tfrac{1}{3}\sin^2\theta_W , \tag{3.11b}$$

$$a_R(u) = T_3(u_R) - \tfrac{2}{3}\sin^2\theta_W , \tag{3.11c}$$

$$a_R(d) = T_3(d_R) + \tfrac{1}{3}\sin^2\theta_W , \tag{3.11d}$$

then from Eqs. (3.9) and (3.10), we get for the left- and right-handed couplings

$$A = \lambda(\tfrac{1}{2} - \sin^2\theta_W + \tfrac{5}{9}\sin^4\theta_W) . \tag{3.12}$$

$$B = \lambda\{[T_3(u_R) - \tfrac{2}{3}\sin^2\theta_W]^2 + [T_3(d_R) + \tfrac{1}{3}\sin^2\theta_W]^2\} . \tag{3.13}$$

Equation (3.12) gives a constraint between λ and $\sin^2\theta_W$. Equation (3.13) represents a circle in the $T_3(u_R) - T_3(d_R)$ plane centered at $(\frac{2}{3}\sin^2\theta_W, -\frac{1}{3}\sin^2\theta_W)$ having radius $(B/\lambda)^{1/2}$. A and B are not known exactly, but are determined by the CDHSB data for R^{ν}, $R^{\bar{\nu}}$, and R_{cc} to be

$$A = 0.282 \pm 0.016 , \qquad B = 0.028 \pm 0.020 . \tag{3.14}$$

For $SU_2 \times SU_2 \times U_1$ models and $SU_3 \times U_1$ models the constraints of the inclusive data are expressed by Eqs. (3.9) and (3.10), writing the couplings $\epsilon_L(u)$, $\epsilon_L(d)$, $\epsilon_R(u)$, and $\epsilon_R(d)$ in terms of the appropriate expressions of Eqs. (2.25)–(2.27).

IV. METHOD AND RESULTS

The five experimental ratios R^{ν}_{e1}, $R^{\bar{\nu}}_{e1}$, R^{ν}, $R^{\bar{\nu}}$ and R_{cc} measured by HPW and CDHSB provide four equations of constraint, Eqs. (2.20), (2.21), (3.9), (3.10), where R^{ν}_{e1}, $R^{\bar{\nu}}_{e1}$, A and B are fixed within experimental errors. We use these four constraints to test various gauge models.

This may be done in a model-independent way by determining limits on the four coupling parameters[20] $\epsilon_L(u)$, $\epsilon_L(d)$, $\epsilon_R(u)$, and $\epsilon_R(d)$. If R^{ν}_{e1}, $R^{\bar{\nu}}_{e1}$, A and B were known exactly, these four couplings would be fixed precisely, aside from sign ambiguities. Experimental errors on the five experimental ratios mean that at best we can determine a range of values for the coupling parameters.

It is useful to introduce a χ^2 function which ex-

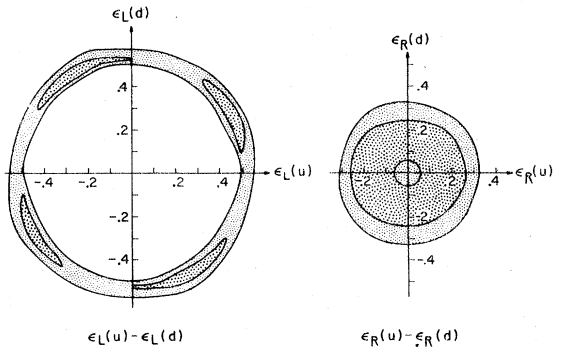

FIG. 3. Constraints on neutral-current coupling parameters due to elastic and deep-inelastic neutral-current data. Figure 3(a) plots left-handed couplings, Fig. 3(b) right-handed couplings. The darker shaded region is consistent within 1 standard deviation, the lighter shaded region within 2 standard deviations.

presses the agreement between model and experiment:

$$\chi^2=\tfrac{1}{4}\left[\left(\frac{R^{\nu}_{e1}(\text{model})-R^{\nu}_{e1}(\text{expt})}{\Delta R^{\nu}_{e1}}\right)^2+\left(\frac{R^{\bar{\nu}}_{e1}(\text{model})-R^{\bar{\nu}}_{e1}(\text{expt})}{\Delta R^{\bar{\nu}}_{e1}}\right)^2+\left(\frac{A(\text{model})-A(\text{expt})}{\Delta A}\right)^2+\left(\frac{B(\text{model})-B(\text{expt})}{\Delta B}\right)^2\right], \tag{4.1}$$

where the denominators ΔR^{ν}_{e1}, $\Delta R^{\bar{\nu}}_{e1}$, ΔA, and ΔB represent 1 standard deviation in the experimentally measured quantities, including both systematic and statistical errors. We can require general agreement within one standard deviation of the four measured quantities by requiring $\chi^2 \leq 1$. This is slightly more lenient than demanding that each constraint be satisfied separately within 1 standand deviation. Agreement within 2 standard deviations of the experimental data (95% confidence level) requires $\chi^2 \leq 4$.

The range of coupling parameters consistent with the elastic and inclusive data within one and two standard deviations is shown in Fig. 3. The figure plots separately left-handed couplings and right-handed couplings, thus ignoring correlations due to the constraints between left- and right-handed coupling parameters. The darker region is the allowed range of couplings within one standard deviation, the lighter region includes coupling values within two standard deviations of the data. Figure 3 reflects an overall sign ambiguity

$$\begin{aligned}&\epsilon_L(u)\longrightarrow-\epsilon_L(u),\\ &\epsilon_L(d)\longrightarrow-\epsilon_L(d),\\ &\epsilon_R(u)\longrightarrow-\epsilon_R(u),\\ &\epsilon_R(d)\longrightarrow-\epsilon_R(d),\end{aligned} \tag{4.2}$$

which cannot be resolved by the neutral-current data.

An important feature of the constraints, namely, the correlations between left- and right-handed couplings, is hidden by Fig. 3. To reveal those correlations, we have plotted the two right-handed couplings, $\epsilon_R(u)$ and $\epsilon_R(d)$, versus a third quantity

$$\theta_L=\tan^{-1}\frac{\epsilon_L(d)}{\epsilon_L(u)}. \tag{4.3}$$

This quantity distinguishes the isoscalar or isovector nature of the left-handed quarks; the couplings are mainly isoscalar for $0\leq\theta_L\leq\pi/2$, mainly isovector for $\pi/2\leq\theta_L\leq\pi$. The fourth parameter, $R_L=[\epsilon_L{}^2(u)+\epsilon_L{}^2(d)]^{1/2}$, is not plotted, but is allowed to vary over all possible values. In practice, R_L is constrained to a small range of values by the inclusive data, $0.51\leq R_L\leq 0.54$ within our one standard deviation criterion, $0.47\leq R_L\leq 0.58$ within the two standard deviation criterion. The correlations among θ_L, $\epsilon_R(u)$, and $\epsilon_R(d)$ are shown in Fig. 4. Again, the dark regions represent parameter values within one standard deviation, the lighter boxed regions give parameter values within two standard deviations of the data.

Seghal,[6] Hung and Sakurai,[7] and Abbott and Barnett[5] have shown that the coupling parameters may be further restricted by including model-dependent constraints coming from inclusive and exclusive single-pion data.

We would like to emphasize that strong constraints are imposed on gauge models without going beyond the new elastic and deep-inelastic neutral-current data. For $SU_2\times U_1$ models, we assume the left-handed u and d quarks have the doublet assignment of Eq. (1.3). This does not fix $\epsilon_L(u)$ or $\epsilon_L(d)$, since λ and $\sin^2\theta_W$ are still free to vary, but it serves to resolve the overall sign ambiguity of Eq. (4.2). The four parameters $T_3(u_R)$, $T_3(d_R)$, $\sin^2\theta_W$, and λ are left free to vary. The values of $T_3(u_R)$, $T_3(d_R)$ and $\sin^2\theta_W$, consistent with the elastic and inclusive data are shown in Fig. 5. The darker regions denote consistency within 1 standard deviation, the lighter boxes within 2 standard deviations. The results indicate that within this broad class of $SU_2\times U_1$ models, only the Weinberg-Salam model $[T_3(u_R)=T_3(d_R)=0]$ is consistent within 1 standard deviation. The Weinberg angle for the WS model ranges from 0.2 to 0.3, and λ, though not plotted, ranges from 0.85 to 1.15, with $\sin^2\theta_W=\frac{1}{4}$, $\lambda=1$ being the preferred values.

Both the b-quark $[T_3(u_R)=\frac{1}{2}, T_3(d_R)=0]$ and t-quark $[T_3(u_R)=0, T_3(d_R)=-\frac{1}{2}]$ models are beyond 2 standard deviations of the experimental data. The vector model $[T_3(u_R)=\frac{1}{2}, T_3(d_R)=-\frac{1}{2}]$, as well as a wide range of less conventional models, is ruled out by the data. One may also construct $SU_2\times U_1$ models in which right-handed u and d quarks occur as mixtures of singlets and doublets. Figure 5 may be used to read off the mixing angles and Weinberg angles consistent with the elastic and inclusive neutral-current data.

The $SU_2\times SU_2\times U_1$ model of Mohapatra and Sidhu depends on the two free parameters ϵ and x. The range of these parameters consistent with the four experimental constraints is shown in Fig. 6. Note that the region preferred by the data centers

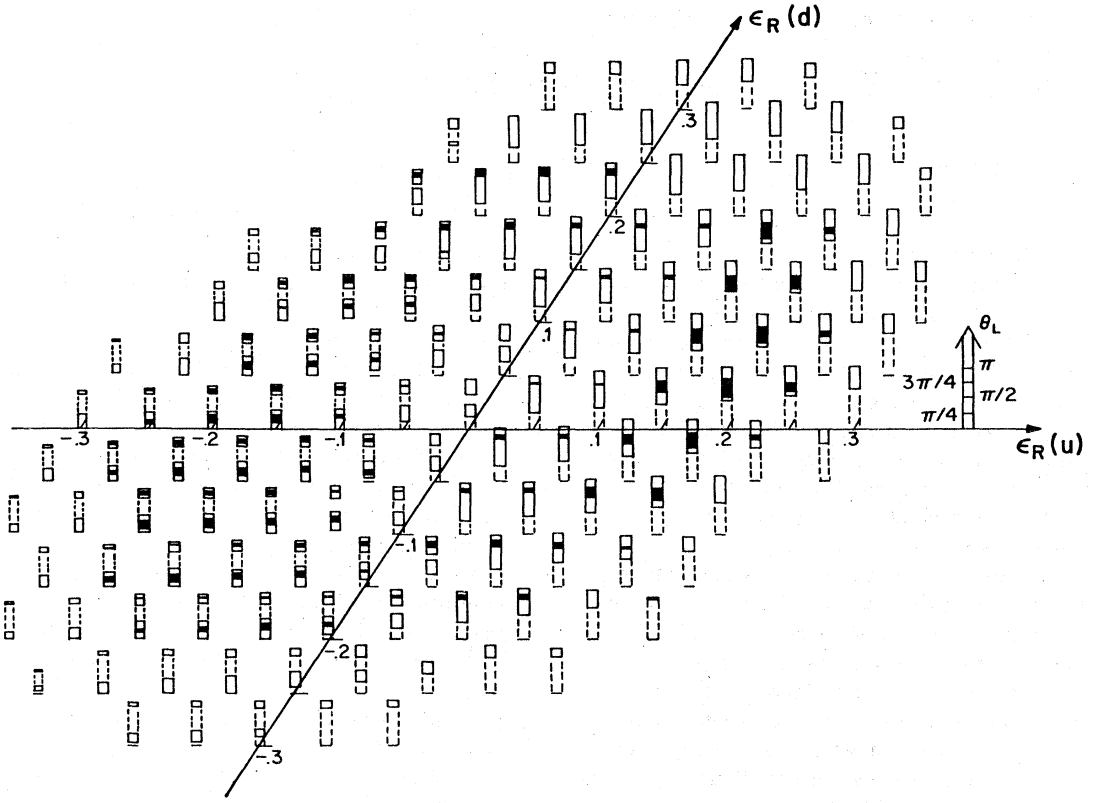

FIG. 4. A three-dimensional plot of constraints on the coupling parameters due to elastic and inclusive neutral-current data. The values of $\epsilon_R(u)$, $\epsilon_R(d)$, and $\theta_L = \tan^{-1}[\epsilon_L(d)/\epsilon_L(u)]$ within 1 standard deviation are shown by the darker regions the values within 2 standard deviations by the lighter boxes. A fourth arbitrary parameter, R_L, is varied over its complete range, but is not plotted here.

around $\epsilon = 0$, the value reproducing the elastic and inclusive phenomenology of the WS $SU_2 \times U_1$ model.

Two $SU_3 \times U_1$ models are less compatible with the data. The Langacker-Segrè model has no choice of parameters compatible within 3 standard deviations of the data, at a χ^2 of 9.7 the preferred parameters values are $r' = 0.95, r'' = 0.55$. The model of Lee and Weinberg has no choice of parameters within 1 standard deviation, but a reasonable range of the two parameters l and w within 2 standard deviations, as shown in Fig. 7.

The conclusions of the preceding analysis are insensitive to several of the assumptions going into the analysis. In particular, the same qualitative conclusions prevail when the parameters k and M_A^2 [Eqs. (2.12) and (2.13)] going into the elastic scattering analysis are allowed separately to vary within 20–30% of their chosen values.

We should also stress the fact that since we have not used the data on the inclusive or exclusive pion productions, the constraints on the coupling parameters are not as strong as those obtained in the previous analyses where these pion productions are included with additional model-dependent assumptions about the pion-production mechanism. However, for the purpose of testing specific gauge models, our analysis shows that the new elastic and deep-inelastic neutral-current data can provide very useful constraints which are free of the model-dependent assumptions on the pion-production mechanism.

V. CONCLUSIONS

The recent elastic (HPW) and deep-inelastic (CDHSB) neutrino induced neutral-current data, used alone and with minimal theoretical assumptions, impose stringent constraints on viable gauge models. Within $SU_2 \times U_1$ models making the usual assignment of left-handed u and d quarks and without mixing of right-handed u and d quarks, only the Weinberg-Salam model is consistent with the data. In the WS $SU_2 \times U_1$ model, the data are consistent with $0.2 \leq \sin^2\theta_W \leq 0.3$ and $0.85 \leq \lambda \leq 1.15$. All other such $SU_2 \times U_1$ models are inconsistent

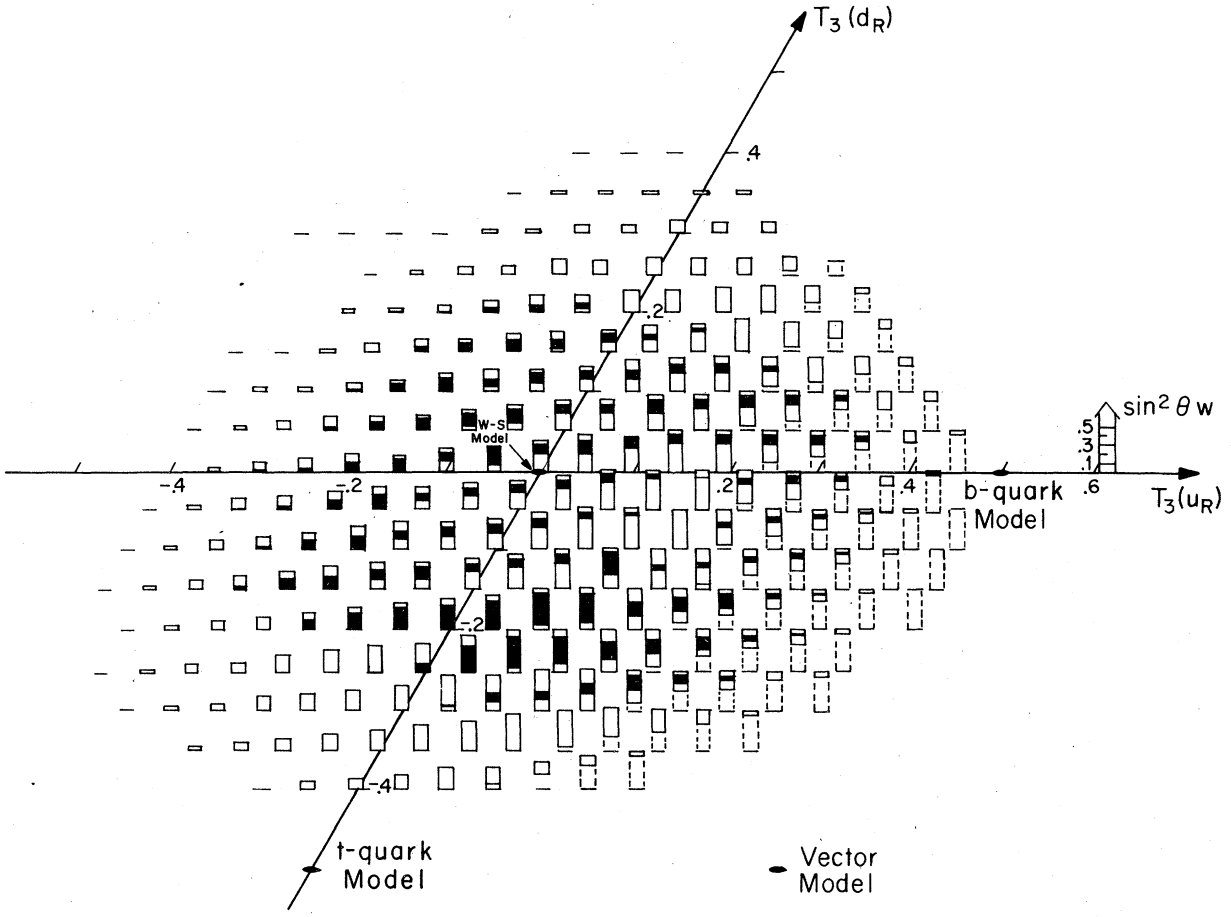

FIG. 5. A three-dimensional plot of constraints on $SU_2 \times U_1$ models due to neutral-current data. The values of $T_3(u_R)$, $T_3(d_R)$, and $\sin^2\theta_W$ consistent within 1 standard deviation of the data are shown by the darker shaded regions; the values within 2 standard deviations are shown by lighter boxed regions. A fourth arbitrary parameter, λ, is varied over its allowed range, but is not plotted in this figure.

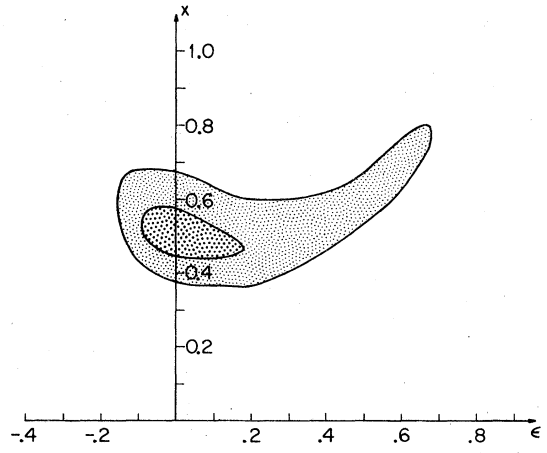

FIG. 6. Values of the $SU_2 \times SU_2 \times U_1$ parameters ϵ and x consistent with elastic and deep-inelastic neutral-current data within 1 standard deviation (darker region) and 2 standard deviations (lighter region).

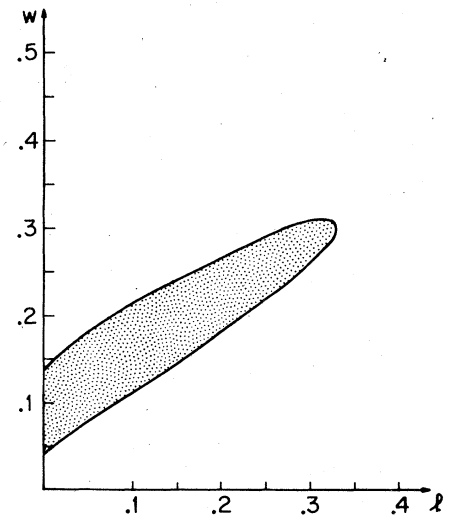

FIG. 7. Values of the Lee-Weinberg $SU_3 \times U_1$ model parameters l and w consistent with the elastic deviations. No choice of parameters falls within 1 standard deviation of the data.

with the data. The parity-conserving $SU_2 \times SU_2 \times U_1$ model of Mohapatra and Sidhu is also consistent with the data for $\epsilon = 0, 0.45 \leq x \leq 0.58$. The $SU_3 \times U_1$ model of Langacker and Segre is not compatible within 3 standard deviations of the recent data, while the $SU_3 \times U_1$ model of Lee and Weinberg falls within 2 standard deviations of the data for certain values of its two adjustable parameters.

ACKNOWLEDGMENTS

We thank Professor F. Messing, Professor L. Sulak, Dr. J. Strait, and Dr. W. Koznecki for discussions on the experimental results. We are especially grateful to Professor L. Wolfenstein for a number of valuable discussions and comments. This work was supported in part by the U. S. Department of Energy.

---

*Permanent address: Physics Department, St. Bonaventure University St. Bonaventure, New York, 14778.

[1]F. J. Hasert *et al.*, Phys. Lett. 46B, 121 (1973); A. Benvenuti *et al.*, Phys. Rev. Lett. 32, 800 (1974).

[2]S. Weinberg, Phys. Rev. Lett. 19, 1264 (1967); A. Salam, in *Elementary Particle Theory: Relativistic Groups and Analyticity (Nobel Symposium No. 8)*, edited by N. Svartholm (Almqvist and Wiksell, Stockholm, 1968). See also E. S. Abers and B. W. Lee, Phys. Rep. 9, 1 (1973); S. Weinberg, Rev. Mod. Phys. 46, 255 (1974); J. C. Taylor, *Gauge Theories of Weak Interactions*, (Cambridge University Press, New York, 1976).

[3]J. B. Strait, Ph.D. thesis, Harvard University, 1978 (unpublished); W. Koznecki, Ph.D. thesis, Harvard University, 1978 (unpublished). For the first generation results, see D. Cline *et al.*, Phys. Rev. Lett. 37, 252 (1976); 37, 648 (1976).

[4]M. Holder *et al.*, Phys. Lett. 72B, 254 (1977). For first results, see W. von Donink, in *Proceedings of the International Neutrino Conference, Aachen, 1976*, edited by H. Laissner, H. Reither, and P. Zerwas (Vieweg, Braunschweig, West Germany, 1977), p. 267; J. Blietschau *et al.*, Nucl. Phys. B118, 218 (1977).

[5]L. F. Abbott and R. Michael Barnett, Phys. Rev. Lett. 40, 1303 (1978).

[6]L. M. Sehgal, Nucl. Phys. B90, 471 (1975); J. Cleymans and L. M. Sehgal, *ibid.* 74, 285 (1974); L. M. Sehgal, Phys. Lett. 71B, 99 (1977).

[7]P. Q. Hung and J. J. Sakurai, Phys. Lett. 72B, 208 (1977).

[8]P. Langacker and D. P. Sidhu, Phys. Lett. 74B, 233 (1978).

[9]See also earlier analyses: C. H. Albright, C. Quigg, R. E. Schrock, and J. Smith, Phys. Rev. D 14, 1780 (1976); D. P. Sidhu, *ibid.* 14, 2235 (1976); V. Barger and D. Nanopoulos, Phys. Lett. 63B, 168 (1976); R. M. Barnett, Phys. Rev. D14, 2990 (1976); T. Hagiwara and E. Takasugi, Phys. Rev. D 15, 89 (1977); J. D. Bjorken, in *Proceedings of the 1976 Summer Institute on Particle Physics*, edited by Martha C. Zipf (SLAC, Stanford, 1976), p. 1.

[10]H. Kluttig *et al.*, Phys. Lett. 71B, 446 (1977); L. M. Seghal, *ibid.* 71B, 99 (1977); P. Q. Hung, *ibid.* 69B, 216 (1977).

[11]W. Krenz *et al.*, Nucl. Phys. B135, 45 (1978); S. L. Adler, Ann. Phys. (N.Y.) 50, 189 (1968); Phys. Rev. D 12, 2644 (1975); S. L. Adler *et al.*, *ibid.* 12, 3501 (1975).

[12]See Bjorken, Ref. 9.

[13]R. N. Mohapatra and D. P. Sidhu, Phys. Rev. Lett. 38, 665 (1977); Phys. Rev. D 16, 2843 (1976). See also H. Fritzsch and P. Minkowski, Nucl. Phys. B103, 61 (1976).

[14]B. W. Lee and S. Weinberg, Phys. Rev. Lett. 38, 1237 (1977).

[15]P. Langacker and G. Segrè, Phys. Rev. Lett. 39, 259 (1977); P. Langacker, G. Segrè, and M. Golshani, Phys. Rev. D 17, 1402 (1978); R. M. Barnett and L. N. Chang, Phys. Lett. 72B, 233 (1977).

[16]W. A. Mann *et al.*, Phys. Rev. Lett. 31, 844 (1973).

[17]See, for example, C. H. Albright *et al.*, Ref. 9.

[18]K. Kleinknecht, in *Proceedings of the 17th International Conference on High Energy Physics, London*, 1974, edited by J. R. Smith (Rutherford Laboratory, Chilton, Didcot, Berkshire, England, 1974), p. III-23.

[19]The γ and γ spectra come from Monte Carlo calculations based on parameterizations of π and κ spectra from p-Be scattering between and 10 and 34 GeV. T. Tso, BNL Report Nos. 11299 JRS/CLW-1 and JRS/CLW-2 (unpublished); see also D. P. Sidhu, Phys. Rev. D 14, 2235 (1976).

[20]The values ϵ_i have absorbed the λ coupling parameters: $\epsilon_i = \lambda^{1/2} a_i$. Thus Eqs. (2.20), (2.21), (3.7)–(3.10) may be written in terms of ϵ_i without the λ factors.

[21]This ratio is measured for $30 \leq E_\nu \leq 90$ GeV; we have assumed the same ratio and error for the full range of inclusive data.